Separation Science and Technology
Publication details, including instructions for authors and subscription information:
http://www.informaworld.com/smpp/title~content=t713708471

Biodegradation Phenomena during Soil Vapor Extraction: A High-Speed Nonequilibrium Model

CÉSAR Gómez-Lahoz[a]; J. M. Rodríguez-Maroto[a]; D. J. Wilson[b]
[a] DEPARTMENTO DE INGENIERÍ QUÍMICA, UNIVERSIDAD DE MÁLAGA, MÁLAGA, SPAIN [b] DEPARTMENT OF CHEMISTRY, VANDERBILT UNIVERSITY, NASHVILLE, TENNESSEE, USA

To cite this Article Gómez-Lahoz, CÉSAR , Rodríguez-Maroto, J. M. and Wilson, D. J.(1994) 'Biodegradation Phenomena during Soil Vapor Extraction: A High-Speed Nonequilibrium Model', Separation Science and Technology, 29: 4, 429 — 463
To link to this Article: DOI: 10.1080/01496399408002155
URL: http://dx.doi.org/10.1080/01496399408002155

SEPARATION SCIENCE AND TECHNOLOGY, **29**(4), pp. 429–463, 1994

Biodegradation Phenomena during Soil Vapor Extraction: A High-Speed Nonequilibrium Model

CÉSAR GÓMEZ-LAHOZ and J. M. RODRÍGUEZ-MAROTO
DEPARTAMENTO DE INGENIERÍA QUÍMICA
UNIVERSIDAD DE MÁLAGA
29071 MÁLAGA, SPAIN

D. J. WILSON*
DEPARTMENT OF CHEMISTRY
VANDERBILT UNIVERSITY
NASHVILLE, TENNESSEE 37235, USA

ABSTRACT

A mathematical model of the biodegradation processes occurring during remediation of contaminated soils by soil vapor extraction (SVE) is presented. The model includes Monod kinetics for biodegradation and rate-limited mass transfer between the aqueous and the gas phases. These mass transfer limitations appear to explain the major features observed in field results presented in the literature: zero-order kinetics with respect to biomass and contaminant, and a very important increase in the percentage contribution of biodegradation to cleanup with decreasing gas flux. Microcomputer runs with the "exact" algorithm are very time-consuming so faster algorithms have been developed using several approximations. These result in savings of more than 95% in computation time, with errors due to the approximations of less than 1%.

INTRODUCTION

Recent studies (1) have estimated the cost for remediation of hazardous waste sites in the United States as around one trillion dollars during the

* To whom correspondence should be sent. Address for August 1993–July 1994: Departamento de Ingeniería Química, Facultad de Ciencias, Universidad de Málaga, Campus Universitario de Teatinos, 29071 Málaga, Spain.

next 30 years. This massive cost makes research on more efficient and economical remediation technologies a priority within the Superfund program. Figure 1 (2) shows the number of times various technologies appear on the Records of Decision (RODs) at the National Priorities List (NPL) sites, and may be considered as a measure of the development, efficiency, and acceptance of the various innovative technologies. Soil vapor extraction (SVE) accounts for almost one-third (31 RODs) of the listings of innovative technologies; bioremediation follows, having been chosen in 22 RODs.

SVE (3, 4) is applicable for the removal of volatile contaminants from the vadose zone of soils having sufficient permeability. It is preferred to the so-called conventional methods, especially in those cases where excavation is not practicable or in which a large area and depth have been contaminated. Basically, SVE consists in drawing clean air through the contaminated soil by means of vacuum wells. Contaminants, which may be in four different phases in the soil (vapor, aqueous solution, nonaqueous phase liquids, and adsorbed to solids), are removed as the contaminant-laden vapor phase is replaced with incoming air and equilibrium is reapproached among the phases.

Bioremediation (5–8) may be performed in situ at sites containing contaminants (both in the vadose and the saturated zones) which are biodegradable. Usually indigenous bacteria are used and the necessary nutrients are supplied to achieve contaminant degradation at a reasonable rate. Although anaerobic biodegradation may also be considered, it usually takes place at a relatively slow rate and may lead to products more toxic than the parent compounds. Thus, an important limiting factor in the subsurface may be dissolved oxygen. Therefore, SVE may promote biodegradation in the unsaturated zone, making SVE technology applicable to compounds which are easily biodegradable even if they are not highly volatile. Furthermore, the overall cost of the process may be reduced if contaminants are destroyed by microorganisms rather than stripped and then separated from air by subsequent treatments (usually activated carbon adsorption or catalytic combustion) which may account for 50% of the total SVE cleanup costs.

Some work has been presented on field applications of SVE where the biodegradation contribution to the cleanup process has been reported to reach values between 15 and 25% (9–11). Hinchee and his collaborators (12, 13) used a SVE design modified to optimize the biodegradation contribution; they have reported up to 85–90% biodegradation. Hogg et al. (14) reported on the successful use of bioremediation at a hydrocarbon-contaminated site in New Zealand; the degradation rate was zero order in hydrocarbon, and oxygen supply was the critical factor in the rate of the

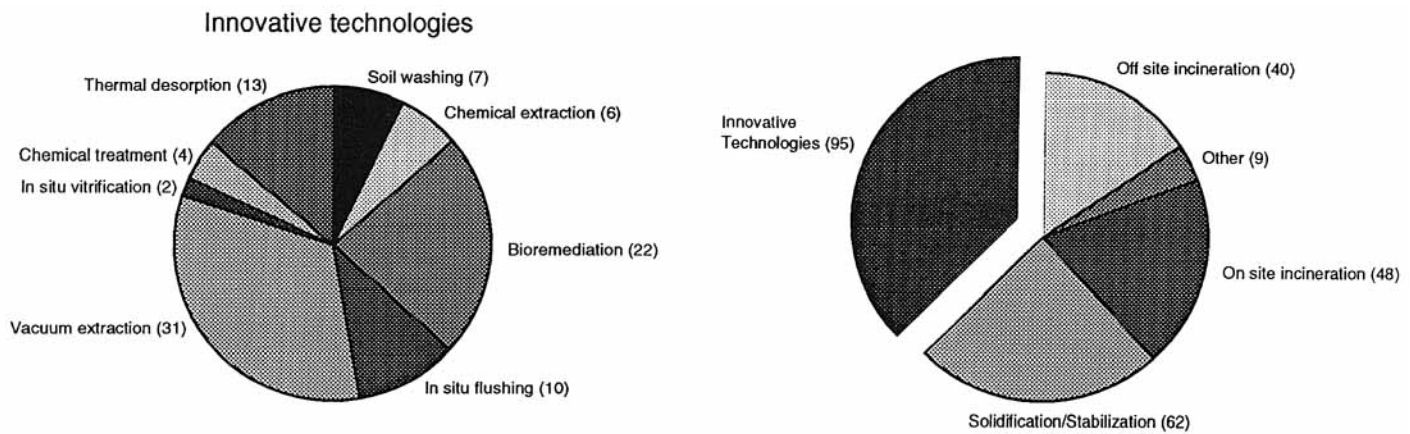

FIG. 1 Summary of innovative vs established treatment technologies at Superfund sites. Data derived from 1982–1989 RODs (2).

process. Average reduction in soil petroleum hydrocarbon concentration was 92% in the course of 13 months.

Although extensive mathematical modeling has been done on SVE (4, 15), to the knowledge of the authors there is at present substantially less modeling on how the biodegradation processes and SVE couple together. Some mathematical work has been presented dealing with biodegradation processes; this is focused mainly on the saturated zone. Borden and Bedient (16) developed a one-dimension model using Monod kinetics to describe the aerobic biodegradation processes occurring in the saturated zone. They also included advection, dispersion, and adsorption terms for oxygen, contaminants, and microorganisms. One of their conclusions was that in those situations in which groundwater is not moving rapidly and the contaminant is not refractory to biodegradation, oxygen transport is controlling and the biological processes may be considered to occur as if all the oxygen available is used instantaneously to oxidize the contaminants to CO_2 and H_2O. They use this approximation in a two-dimensional model which shows the important effect of biodegradation on contaminant concentration and distribution in the plume.

MacQuarrie et al. (17) used a "principal direction" Galerkin finite element technique to solve the two-dimensional model without introducing Borden's assumption of instantaneous reaction and reached very similar results. Widdowson et al. (18, 19) developed a model which considers NO_3^- and O_2 as electron acceptors for the biodegradation process. Monod kinetics are also used with the introduction of a noncompetitive inhibition term for nitrate utilization in the process of oxygen.

Sleep and Sykes (20) developed a model which considered three-phase (air–organic–water) flow and transport and an arbitrary number of components in each phase. Sorption effects between aqueous and solid phases are included. Henry's law is used to relate concentrations between phases. A spill of toluene is simulated with contaminant present in the saturated and the unsaturated soil, and results are shown with and without inclusion of biodegradation. Simplified Monod kinetics are used. Substantial variation in the contaminant concentration contours is observed in the unsaturated and upper saturated zones, but not deep below the water table. Air and oxygen injection in the unsaturated soil were studied and found to further modify the concentration contours of the unsaturated zone, but to leave the lower part of the plume almost unchanged.

Semprini and McCarty (21) developed a model in which contaminants and electron donor and acceptor are transported by advection and dispersion with linear adsorption phenomena, whereas biomass is assumed to be an attached immobile thin biofilm that is fully penetrated by substrate with no mass transfer limitations. The model reproduces fairly well the

field results obtained during field biostimulation of methanotrophic bacteria. These authors published a later paper (22) on the cometabolic transformation of chlorinated aliphatic compounds by methanotrophic bacteria, considering some competitive inhibition of the substrates.

Other models for describing biodegradation in the vadose include the VIP model developed at Utah State University, the RITZE model developed at EPA's Kerr Laboratory in Ada, Oklahoma, and a bioventing model which has been developed for Battelle Northwest.

MODEL FOR BIODEGRADATION AND VAPOR EXTRACTION

Monod kinetics is widely used for the description of microbiological processes in the subsoil, and is chosen here, too. SVE processes are based on the creation of a pressure gradient in the soil that produces relatively fast movement of the vapor phase. Some of the field results reported for biodegradation processes during SVE (11, 23) indicate that the biodegradation rate seem to be zero order with respect to contaminant and biomass concentrations, which allows one to consider oxygen as the limiting factor for biodegradation. On the other hand, the oxygen concentration in the vapor phase is reported to be relatively high, and air flow through the domain should lead to a higher biodegradation contribution. Since mass transfer limitations are widely found during contaminant removal with SVE (making pulse venting an interesting option), the proposed model includes nonequilibrium oxygen transport from the vapor to the aqueous phase. The model considers advective movement of oxygen and contaminant in the vapor phase, and an immobile aqueous phase which contains oxygen and the contaminant which are not necessarily in equilibrium with the vapor phase. Although nonequilibrium effects are likely to be due to intra-aggregate diffusion, it is considered more practical to use a simple lumped-parameter first-order mass transfer (24).

In addition to including these transport processes, it has been tried to develop a model which is as flexible as possible from the biological point of view to allow several sensitivity studies. Some of the features included are 1) an indefinite number of nutrient terms (with these nutrients considered to be present only in the aqueous phase), and 2) the possible presence of a second substrate which can be volatile or nonvolatile and which can act as a competitive inhibitor of the utilization of the first substrate or even as a toxin to the biomass population. Although biomass is usually considered to be adsorbed onto the solids of the aquifer, with only a small portion moving (floating freely or attached to very small particles) with the aqueous phase, here it is considered as if it were in the aqueous phase.

No net effect should be produced in the overall transport equations, since the model does not include aqueous phase movement, and the fully penetrated biofilm assumed by Semprini and McCarty (21) allows one to neglect the diffusion terms for the transport of substrate and oxygen into the biomass. The model assumes a one-dimensional column geometry, with the column partitioned into a series of compartments (horizontal slabs) for analysis.

The rather extensive list of symbols used in the model is as follows.

A_z = concentration of zth nutrient (g/cm^3 of aqueous phase)
B = biomass (g/cm^3 of aqueous phase)
C_j^s = contaminant j (j = 1, 2) concentration in the nonadvective phases (g/cm^3 of aqueous phase)
C_j^v = contaminant j (j = 1, 2) concentration in vapor phase (g/cm^3 of vapor phase)
C_2^* = threshold value of the concentration of contaminant 2 for toxic effects on biomass (g/cm^3 of aqueous phase)
F = acute toxicity exponential factor for contaminant 2 (dimensionless)
K_B = die-off coefficient for microorganisms (s^{-1})
K_{B_0} = die-off coefficient in the absence of toxic compounds (s^{-1})
K_{Cj} = contaminant j (j = 1, 2) half-saturation constant (g/cm^3)
K_D = Darcy's constant, pore basis (cm^3/atm·s). (Volumetric flow rate of air per unit area = $-\nu K_D \nabla P$)
K_j = nutrient j half-saturation constant (g/cm^3)
Kh_{Cj} = Henry's constant of contaminant j (j = 1, 2) (dimensionless)
Kh_O = Henry's constant of oxygen (dimensionless)
K_{max} = maximum rate of growth of biomass on the best of substrates (s^{-1})
K_O = oxygen half-saturation constant (g/cm^3)
n_j = stoichiometric coefficient for contaminant j (j = 1, 2) (g of contaminant j required to produce 1 g of new biomass)
$n_{O,j}$ = stoichiometric coefficient for oxygen with contaminant j (j = 1, 2) (g of oxygen required to produce 1 g of new biomass with contaminant j)
n'_O = stoichiometric coefficient for endogenous respiration (g of oxygen consumed per g of dead biomass)
$n_{z,j}$ = stoichiometric coefficient for nutrient z for contaminant j (j = 1, 2) (g of free nutrient z required to produce 1 g of new biomass)
n'_z = stoichiometric coefficient for release of nutrient z after biomass die-off (g of nutrient released from 1 g of dead biomass)
O^s = oxygen concentration in aqueous phase (g/cm^3 of aqueous phase)
O^v = oxygen concentration in vapor phase (g/cm^3 of vapor phase)

t = time (s)
v = pore velocity of air in porous medium (cm/s)
x = distance along the column from the gas input (cm)
α_j = relative maximum growth rate of biomass on contaminant j (j = 1, 2) relative to the best substrate (dimensionless)
λ_{Cj} = mass transfer rate coefficient for contaminant j (j = 1, 2) through water film (s^{-1})
λ_O = mass transfer rate coefficient for oxygen through water film (s^{-1})
ν = air-filled void fraction of soil (dimensionless)
ω = volumetric moisture fraction of soil (dimensionless)

The modeling equations are as follows.

The rate of change of biomass per unit volume is assumed to be given by

$$\frac{\partial B}{\partial t} = K_{max} B \frac{\alpha_1 \dfrac{C_1^s}{K_{C1}} + \alpha_2 \dfrac{C_2^s}{K_{C2}}}{1 + \dfrac{C_1^s}{K_{C1}} + \dfrac{C_2^s}{K_{C2}}} \frac{O^s}{K_O + O^s} \prod_{j=1}^{n} \left[\frac{A_j}{K_j + A_j}\right] - K_B B \qquad (1)$$

Here the first (complex) term represent the growth of biomass by consumption of contaminants, nutrients, and oxygen, while the term $-K_B B$ represents the die-off of microorganisms.

The rate of change of concentration of nutrient i is taken as

$$\frac{\partial A_i}{\partial t} = -K_{max} B \frac{n_{i,1}\alpha_1 \dfrac{C_1^s}{K_{C1}} + n_{i,2}\alpha_2 \dfrac{C_2^s}{K_{C2}}}{1 + \dfrac{C_1^s}{K_{C1}} + \dfrac{C_2^s}{K_{C2}}} \frac{O^s}{K_O + O^s} \prod_{j=1}^{n} \left[\frac{A_j}{K_j + A_j}\right] + n_i' K_B B \qquad (2)$$

The first term represents consumption of nutrient i by the live biomass, while the term $n_i' K_B B$ represents the regeneration of the nutrient by its release from dead biomass.

The rate of change of the oxygen concentration in the aqueous phase is taken as

$$\frac{\partial O^s}{\partial t} = -K_{max} B \frac{n_{O,1}\alpha_1 \dfrac{C_1^s}{K_{C1}} + n_{O,2}\alpha_2 \dfrac{C_2^s}{K_{C2}}}{1 + \dfrac{C_1^s}{K_{C1}} + \dfrac{C_2^s}{K_{C2}}} \frac{O^s}{K_O + O^s} \prod_{j=1}^{n} \left[\frac{A_j}{K_j + A_j}\right] - n_O' K_B B + \lambda_O \left[\frac{O^v}{K h_O} - O^s\right] \qquad (3)$$

The first term represents oxygen consumption for degradation of contaminants by the living microorganisms; the second, the consumption of oxygen by the degradation of dead biomass (endogeneous respiration); the third, the mass transfer of oxygen from the vapor phase to the solution.

The rate of change of concentration of the first contaminant in the stationary phases is represented as

$$\frac{\partial C_1^s}{\partial t} = \lambda_{C1}\left[\frac{C_1^v}{Kh_{C1}} - C_1^s\right] - K_{max}B\frac{\dfrac{n_1\alpha_1\dfrac{C_1^s}{K_{C1}}}{1+\dfrac{C_1^s}{K_{C1}}+\dfrac{C_2^s}{K_{C2}}}\dfrac{O^s}{K_O+O^s}\prod_{j=1}^{n}\left[\dfrac{A_j}{K_j+A_j}\right]}{} \tag{4}$$

Here the first term represents mass transport of the first contaminant between the stationary phase and the vapor phase, and the second term represents destruction of this contaminant by biodegradation. A virtually identical equation, given below, gives the rate of change of concentration of the second contaminant in the stationary phases:

$$\frac{\partial C_2^s}{\partial t} = \lambda_{C2}\left[\frac{C_2^v}{Kh_{C2}} - C_2^s\right] - K_{max}B\frac{\dfrac{n_2\alpha_2\dfrac{C_2^s}{K_{C2}}}{1+\dfrac{C_1^s}{K_{C1}}+\dfrac{C_2^s}{K_{C2}}}\dfrac{O^s}{K_O+O^s}\prod_{j=1}^{n}\left[\dfrac{A_j}{K_j+A_j}\right]}{} \tag{5}$$

Next, the rates of change of the concentrations of the components present in the vapor phase are presented. The vapor phase concentrations of the two contaminants are given by

$$\frac{\partial C_1^v}{\partial t} = -\lambda_{C1}\frac{\omega}{v}\left[\frac{C_1^v}{Kh_{C1}} - C_1^s\right] - \frac{\partial(vC_1^v)}{\partial x} \tag{6}$$

and

$$\frac{\partial C_2^v}{\partial t} = -\lambda_{C2}\frac{\omega}{v}\left[\frac{C_2^v}{Kh_{C2}} - C_2^s\right] - \frac{\partial(vC_2^v)}{\partial x} \tag{7}$$

In these equations the first term is a lumped parameter representation of mass transport between the stationary condensed phases and vapor phase, and the second term represents the effect of advection of gas through the column.

The vapor phase oxygen concentration is assumed to be governed by an equation very similar to the last two; it is

$$\frac{\partial O^v}{\partial t} = -\lambda_O \frac{\omega}{v}\left[\frac{O^v}{Kh_O} - O^s\right] - \frac{\partial(vO^v)}{\partial x} \tag{8}$$

in which the first term represents mass transport of oxygen between the vapor and the stationary phases, and the second term represents the effect of advective transport of oxygen by the moving gas stream.

It was assumed that contaminant 2 could exert a toxic effect on the biomass through an increase in the rate of die-off; this is modeled by means of Eq. (9):

$$K_B = K_{B_0}[1 + (C_2^s/C_2^*)^F] \tag{9}$$

This system of coupled nonlinear partial differential equations was then approximated by a similar system of ordinary differential equations in which the variables were calculated only at a discrete set of values of x:

$$\frac{1}{2}\Delta x, \frac{3}{2}\Delta x, \ldots, \frac{(2n+1)}{2\Delta x}$$

A computer program implementing the model as described above was written in TurboBASIC, and computations were carried out on an MMG 286 computer with a math coprocessor and operating at 12 MHz. It was assumed that the initial values of all concentrations were independent of position in the column, and the modeling equations were then integrated forward in time to simulate the bioremediation process.

RESULTS

A first set of runs was performed using the most simplified biological conditions ($C_2 = 0$, $\alpha_1 = 1$, C_1 written simply as C and nutrients present in large excess) for the remediation of a hypothetical site to check the influence of the mass transfer coefficients on the cleanup time and the biodegradation contribution. It was also assumed that no endogenous respiration occurred ($n'_O = 0$). This permits Eqs. (1) through (9) to be replaced by Eqs. (10) through (14).

$$\frac{\partial B}{\partial t} = K\frac{O^s}{K_O + O^s}\frac{BC^s}{K_C + C^s} - K_B B \tag{10}$$

$$\frac{\partial C^v}{\partial t} = -\lambda_C \frac{\omega}{v}\left(\frac{C^v}{Kh_C} - C^s\right) - \frac{\partial(vC^v)}{\partial x} \tag{11}$$

$$\frac{\partial O^v}{\partial t} = -\lambda_O \frac{\omega}{v}\left(\frac{O^v}{Kh_O} - O^s\right) - \frac{\partial(vO^v)}{\partial x} \tag{12}$$

$$\frac{\partial C^s}{\partial t} = \lambda_C\left[\frac{C^v}{Kh_C} - C^s\right] - n_C K \frac{O^s}{K_O + O^s}\frac{BC^s}{K_C + C^s} \tag{13}$$

$$\frac{\partial O^s}{\partial t} = \lambda_O\left[\frac{O^v}{Kh_O} - O^s\right] - n_O K \frac{O^s}{K_O + O^s}\frac{BC^s}{K_C + C^s} \tag{14}$$

Since these equations are still coupled and strongly nonlinear, it is necessary to integrate them numerically, which is done by using a discrete (mesh) approximation for the space derivatives in the advection terms. The column is partitioned into N compartments and we write for the ith volume element:

$$C^s\left[\left(i - \frac{1}{2}\right)\Delta x\right] = C_i^s \tag{15}$$

$$B\left[\left(i - \frac{1}{2}\right)\Delta x\right] = B_i \tag{16}$$

$$C^v\left[\left(i - \frac{1}{2}\right)\Delta x\right] = C_i^v \tag{17}$$

and the mass of contaminant in the ith compartment is given by

$$M_i = (vC_i^v + \omega C_i^s)V_i \tag{18}$$

where V_i is the volume (cm^3) of the ith compartment and M_i is in g.

The velocity of the gas coming into the ith compartment is estimated by (25)

$$v_x = \frac{K_D(P_{\text{in}}^2 - P_{\text{out}}^2)\sqrt{P_{\text{in}}^2 - \dfrac{P_{\text{in}}^2 - P_{\text{out}}^2}{L}x}}{2L} \tag{19}$$

where P_{in} is the pressure (atm) at the gas input end of the column, P_{out} is the outlet pressure, K_D is the Darcy's constant for the soil in the column (cm^3/atm·s), x is the distance from the inlet end of the column (cm), and L is the column length (cm). We have

$$\left.\begin{aligned} x &= (i - 1)\Delta x \\ L &= N\Delta x \end{aligned}\right\} \frac{x}{L} = \frac{i - 1}{N} \tag{20}$$

TABLE 1
Values for the Parameters Used in Runs Presented in Figs. 2–16

Column length (L)	50 cm
Column radius (r)	10 cm
Number of volume elements into which the column is partitioned (N)	10
Voids fraction associated with the mobile phase (ν)	0.2
Volumetric moisture content of the soil (ω)	0.2
Inlet pressure (P_{in})	1 atm
Outlet pressure (P_{out})	0.9/0.99 atm
Temperature (T)	15°C
Darcy's constant (K_D)	50 cm^2/atm·s
Soil density (ρ)	1.5 g/cm^3
Initial contaminant concentration ($M/\rho V$)	100 mg contaminant/kg soil
Initial biomass concentration (B)	10^{-3} mg/L
Henry's constant of contaminant (Kh_c)	10^{-3}
Henry's constant of oxygen (Kh_O)	30
Stoichiometric coefficient for substrate (n_c)	2 g substrate/g biomass
Stoichiometric coefficient for oxygen (n_O)	3 g oxygen/g biomass
Maximum velocity constant (K)	$2 \cdot 10^{-5}/0$ s^{-1}
Michaelis constant of substrate (K_c)	0.1 mg/L
Michaelis constant of oxygen (K_O)	0.1 mg/L
Die-off coefficient of biomass (K_B)	10^{-7} s^{-1}

so the input gas velocity to the ith compartment is given by

$$v(i-1) = \frac{K_D(P_{in}^2 - P_{out}^2)}{2L} \sqrt{P_{in}^2 - \frac{P_{in}^2 - P_{out}^2}{N}(i-1)} \qquad (21)$$

Table 1 shows the parameters and starting conditions used in these runs. The biological parameters may be compared to those reported in the literature, summarized in Table 2. The effective mass transfer coeffi-

TABLE 2
Some Biological Parameters Used in the Literature Compared to Those Used in This Work

Parameter	Borden, 1986 (16)	Widdowson, 1988 (18)	Strand, 1988 (33)	MacQuarrie, 1990 (17)	Semprini, 1991 (21)	Dhawan, 1991 (28)	This work
K (s^{-1})	1×10^{-5}	3.6×10^{-5}	2×10^{-5}	1.3×10^{-5}	$2.8–4.6 \times 10^{-5}$	2.78×10^{-5}	2×10^{-5}
n_c (g C/g B)	2	2.22	1	2.35	2.0	2	2
n_O (g O/g B)	6	1.4	2.6	6.2	4.8	1	3
K_c (mg/L)	0.13	40	0.48	0.65	2	1	0.1
K_O (mg/L)	0.10	0.78	0.032	0.1	1	0.01	0.1
K_B (s^{-1})	1.16×10^{-7}	2.3×10^{-7}	—	—	$1.7–1.2 \times 10^{-6}$	2.78×10^{-7}	1×10^{-7}

cients of oxygen (λ_O) and the contaminant (λ_C) are always taken as having a ratio 2:1, which is in good agreement with the corresponding oxygen/organic pollutant diffusivities in water solutions frequently encountered in vapor-stripping applications (26). Runs have been made for λ_C values ranging from 10^{-3} to 10^{-7} s^{-1}. In Figs. 2 to 6 results for these runs are presented as the logarithm of the total contaminant mass versus time for runs with and without biodegradation.

As can be seen from the figures, the theoretical cleanup time to achieve high removal percentages (99.996%) of a volatile organic compound (VOC) when no biodegradation is considered in the model is usually more than twice that resulting when biodegradation is included. Moreover, the time savings which can be ascribed to biodegradation are relatively more important when the mass transfer coefficients are smaller.

These computed results are obtained for an assumed initial biomass concentration which is even lower than that used by Borden and Bedient (16) in their simulations, in which a value [obtained from Lee et al. (27)] of 0.001 mg/L of soil was used. Sleep and Sykes (20) used a starting biomass concentration provided by MacQuarrie et al. (17) of 0.230 mg/L, and Widdowson et al. (18) used a value of 0.565 mg/L which they calcu-

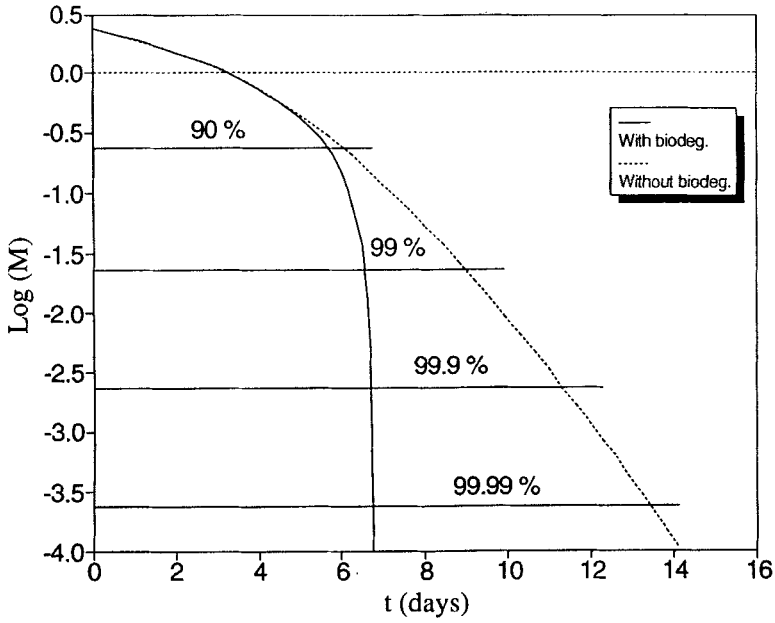

FIG. 2 Cleanup times required with ($K = 2 \times 10^{-5}$ s^{-1}) and without ($K = 0$ s^{-1}) biodegradation. $\lambda_C = 10^{-3}$ s^{-1}; $\lambda_O = 2 \times 10^{-3}$ s^{-1}; M (g). See Table 1 for parameter values; $P_{out} = 0.90$ atm.

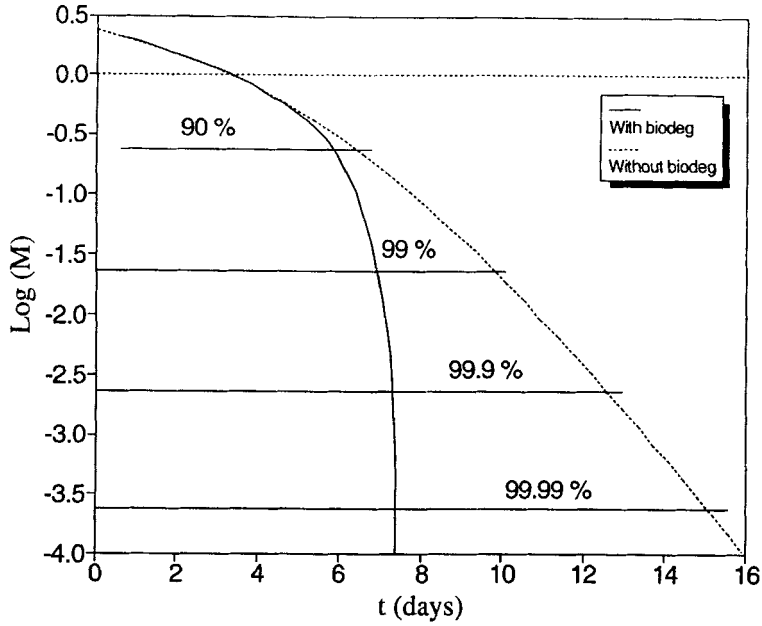

FIG. 3 Cleanup times required with ($K = 2 \times 10^{-5}\ s^{-1}$) and without ($K = 0\ s^{-1}$) biodegradation. $\lambda_C = 10^{-4}\ s^{-1}$; $\lambda_O = 2 \times 10^{-4}\ s^{-1}$; M (g). See Table 1 for parameter values; $P_{out} = 0.90$ atm.

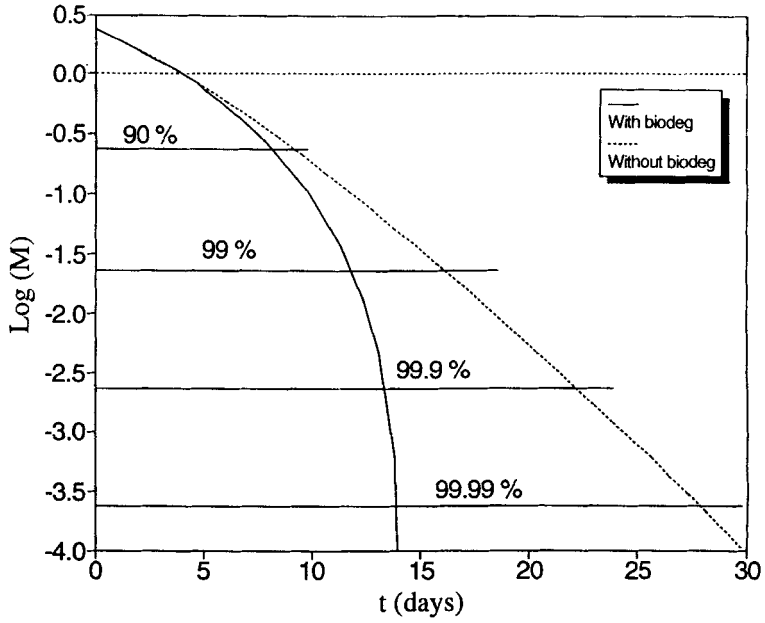

FIG. 4 Cleanup times required with ($K = 2 \times 10^{-5}\ s^{-1}$) and without ($K = 0\ s^{-1}$) biodegradation. $\lambda_C = 10^{-5}\ s^{-1}$; $\lambda_O = 2 \times 10^{-5}\ s^{-1}$; M (g). See Table 1 for parameter values; $P_{out} = 0.90$ atm.

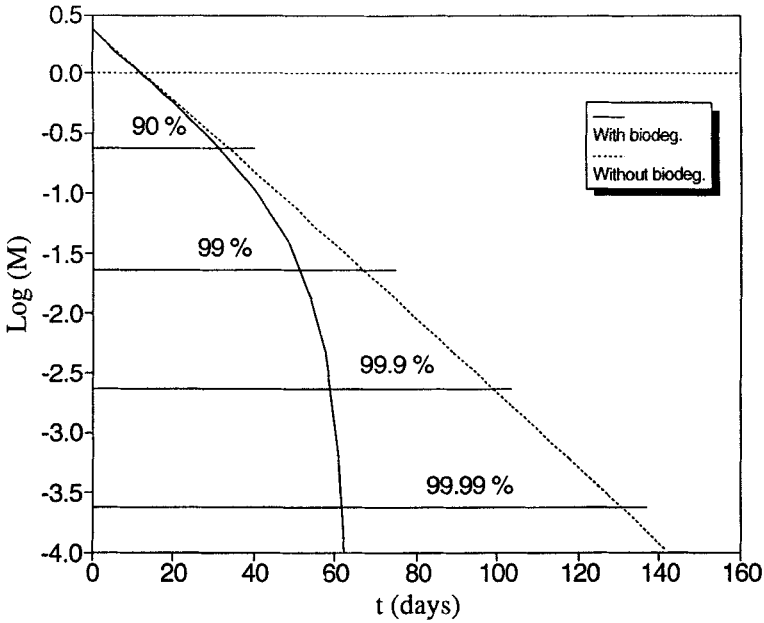

FIG. 5 Cleanup times required with ($K = 2 \times 10^{-5}\ s^{-1}$) and without ($K = 0\ s^{-1}$) biodegradation. $\lambda_C = 10^{-6}\ s^{-1}$; $\lambda_O = 2 \times 10^{-6}\ s^{-1}$; M (g). See Table 1 for parameter values; $P_{out} = 0.90$ atm.

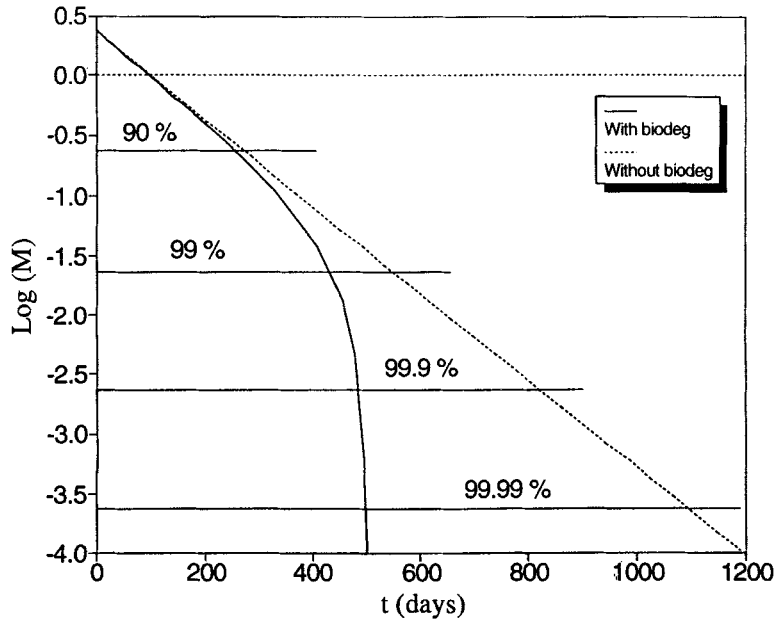

FIG. 6 Cleanup times required with ($K = 2 \times 10^{-5}\ s^{-1}$) and without ($K = 0\ s^{-1}$) biodegradation. $\lambda_C = 10^{-7}\ s^{-1}$; $\lambda_O = 2 \times 10^{-7}\ s^{-1}$; M (g). See Table 1 for parameter values; $P_{out} = 0.90$ atm.

lated to correspond to a starting population of 10^6 cells/g. Semprini and McCarty (22) used a value close to 0.150 mg/L; Dhawan et al. (28) used 0.100 mg/L.

Bossert and Bartha (29) reported typical microbial counts of 10^7 to 10^9/g of soil, with counts of hydrocarbon degraders ranging from 10^5 to 10^6 at sites with no pollution history up to 10^6 to 10^8 if there is a history of pollution. If one assumes an average mass per organism of 1.1×10^{-9} mg [roughly estimated from figures given by McKinney (30) and in reasonably good agreement with the value calculated from Widdowson's data above], a count of 10^6 organisms/g corresponds to a biomass concentration of about 10^{-3} mg/g, or roughly 1 mg/L.

Thus the value of initial biomass concentration used in the calculations described here (0.0002 mg/L of soil) is quite a bit lower than typical literature values. This initial value therefore represents a conservative situation even for most field cases where no inoculation of degrading bacteria is used to enhance bioremediation. Evidently, if even a quite small population of active microorganisms is present and capable of growth on the substrate, biodegradation will develop once aeration by SVE is initiated.

Calculated cleanup times and computer run times for those runs corresponding to Figs. 2 to 6 are presented in Table 3. Runs which do not include biodegradation were made with the same computer program as was used for runs with biodegradation; in the former a value of zero was used for the Monod maximum reaction rate parameter K. It is seen that if biodegradation is not included in the model, the results are quite comparable to the results obtained with biodegradation during the removal of roughly the first 50% of the contaminant, after which biodegradation begins to contribute more and more significantly. See Figs. 2 to 6. Removal of contaminant by vapor stripping alone typically requires at least as much

TABLE 3
Results Obtained for Different Diffusion Constants with the Rigorous Model, With and Without Biodegradation

Biodegradation	λ_O (s^{-1})	λ_C (s^{-1})	Δt (s)	Run time (h)			Theoretical cleanup time (h)		
				50%	99.9%	99.996%	50%	99.9%	99.996%
Yes	2×10^{-7}	10^{-7}	35	6.80	41.18	42.48	1.92×10^3	1.16×10^4	1.20×10^4
No	2×10^{-7}	10^{-7}	35	6.77	67.75	98.73	1.97×10^3	1.97×10^4	2.87×10^4
Yes	2×10^{-6}	10^{-6}	25	1.19	7.05	7.42	2.39×10^2	1.42×10^3	1.49×10^3
No	2×10^{-6}	10^{-6}	25	1.18	11.43	16.48	2.45×10^2	2.37×10^3	3.42×10^3
Yes	2×10^{-5}	10^{-5}	25	0.40	1.59	1.69	8.04×10^1	3.23×10^2	3.37×10^4
No	2×10^{-5}	10^{-5}	25	0.38	2.56	3.46	8.04×10^1	5.32×10^2	7.18×10^2
Yes	2×10^{-4}	10^{-4}	7.5	1.13	3.02	3.11	6.85×10^1	1.83×10^2	1.85×10^2
No	2×10^{-4}	10^{-4}	7.5	1.09	4.84	6.15	6.85×10^1	3.01×10^2	3.83×10^2
Yes	2×10^{-3}	10^{-3}	0.75	11.20	28.72	28.86	6.78×10^1	1.74×10^2	1.75×10^2
No	2×10^{-3}	10^{-3}	0.75	10.88	44.04	55.26	6.78×10^1	2.72×10^2	3.40×10^2

time to go from 90 to 99% removal as is required to remove the first 90% of contaminant. This tailing is even more significant when one uses low values for the mass transfer rate coefficients. Including biodegradation should result in more optimistic and accurate calculations than those resulting from models that do not consider it, especially for the removal of the last 10% or so of the contaminant in the vadose zone.

The runs including biodegradation are separately represented again in Figs. 7 to 11; here the amount of contaminant removed by stripping is compared as a percentage to that removed by biodegradation. For the parameter values used in this series, when remediation is complete the total amount of substrate that has been removed by biodegradation is little changed even when the mass transfer coefficients are changed by four orders of magnitude.

Since the initial amount of biomass is so small, there is an initial period of time during which contaminant removal by biodegradation is negligible. This is the period of time required for the biomass to increase from approximately 1 μg/L to 1 mg/L of aqueous phase. As can be seen from Figs. 7 to 9, this requires 350,000 s (4 days) for those runs. In Figs. 7 and 8 an exponential growth of biodegradation is observed up to the time at which

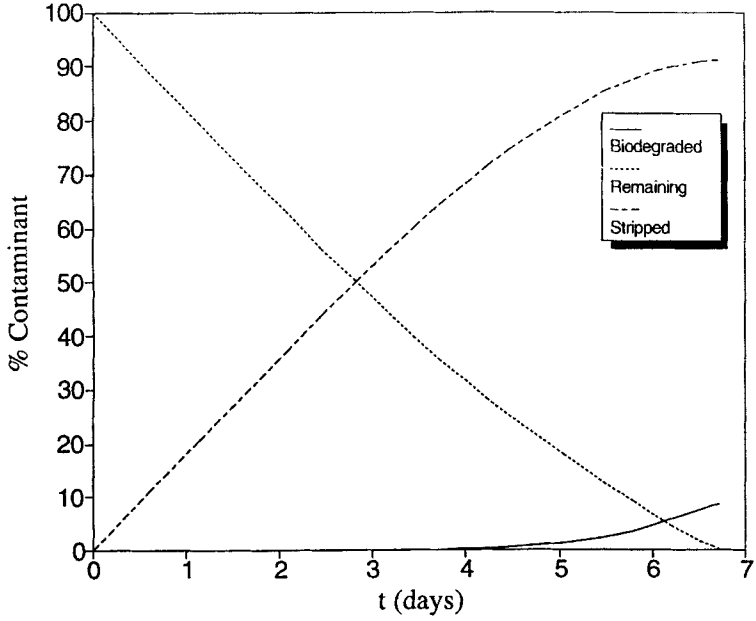

FIG. 7 Percentage of contaminant removal by stripping and biodegradation versus time. $\lambda_C = 10^{-3}\ s^{-1}$; $\lambda_O = 2 \times 10^{-3}\ s^{-1}$. See Table 1 for parameter values; $P_{out} = 0.90$ atm.

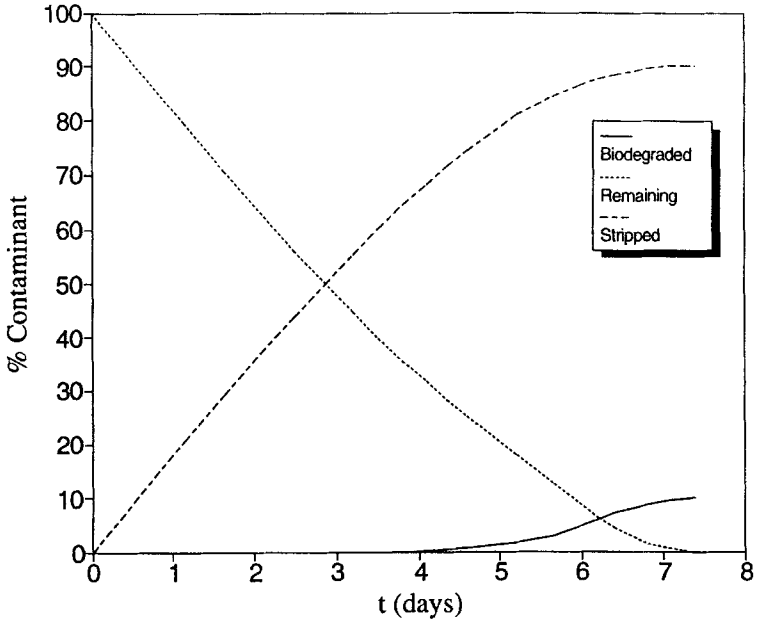

FIG. 8 Percentage of contaminant removal by stripping and biodegradation versus time. $\lambda_C = 10^{-4}\ s^{-1}$; $\lambda_O = 2 \times 10^{-4}\ s^{-1}$. See Table 1 for parameter values; $P_{out} = 0.90$ atm.

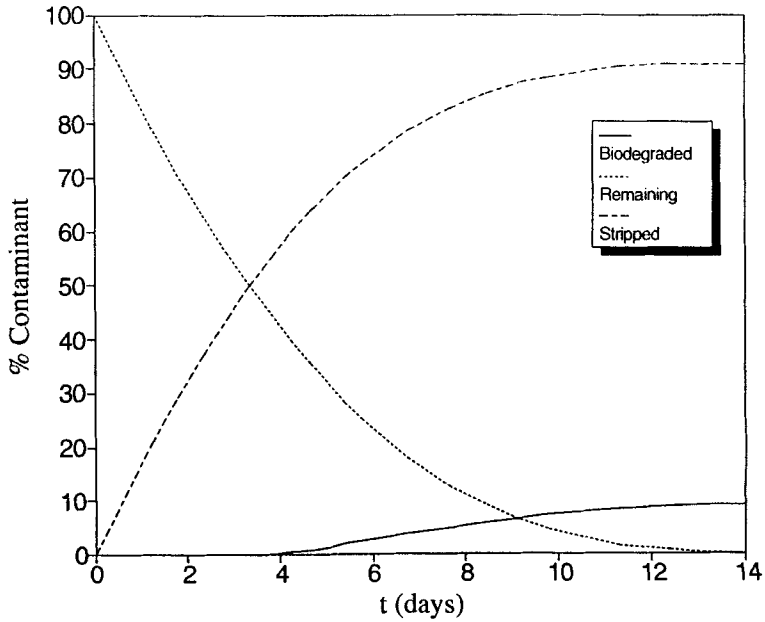

FIG. 9 Percentage of contaminant removal by stripping and biodegradation versus time. $\lambda_C = 10^{-5}\ s^{-1}$; $\lambda_O = 2 \times 10^{-5}\ s^{-1}$. See Table 1 for parameter values; $P_{out} = 0.90$ atm.

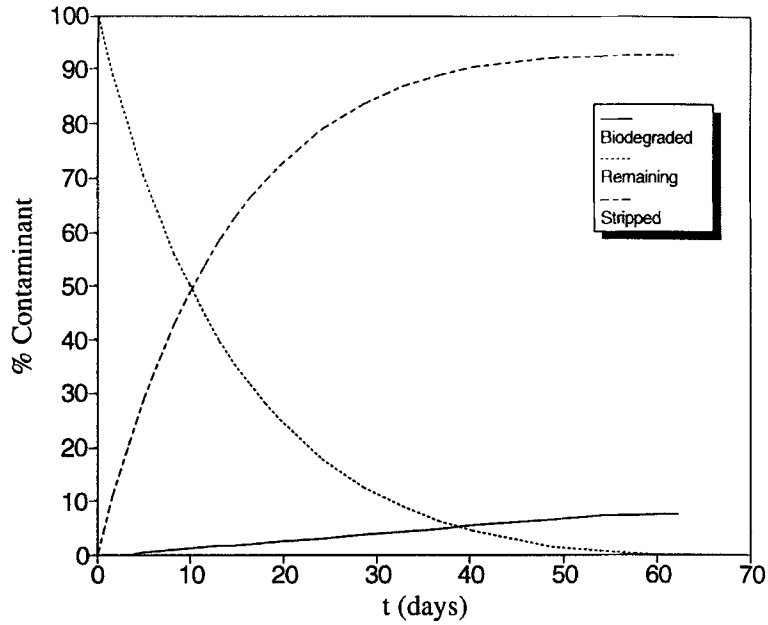

FIG. 10 Percentage of contaminant removal by stripping and biodegradation versus time. $\lambda_C = 10^{-6}\ s^{-1}$; $\lambda_O = 2 \times 10^{-6}\ s^{-1}$. See Table 1 for parameter values; $P_{out} = 0.90$ atm.

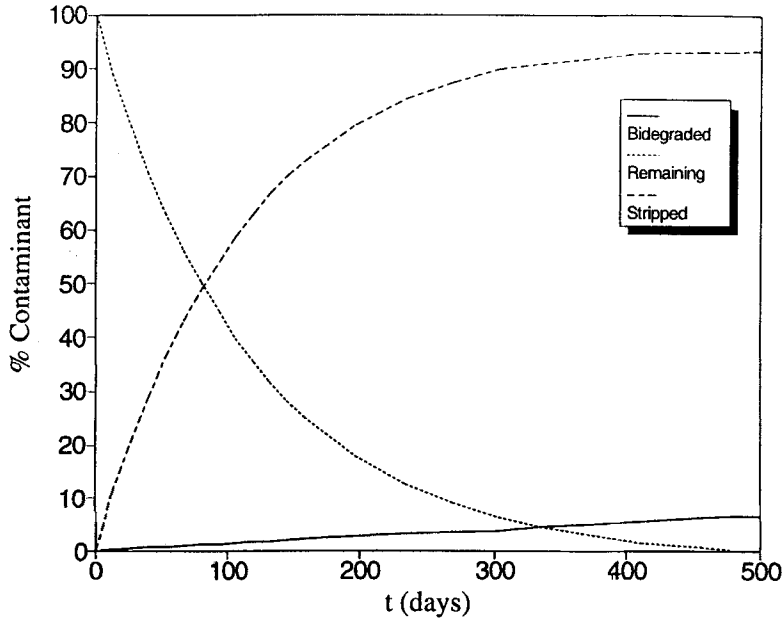

FIG. 11 Percentage of contaminant removal by stripping and biodegradation versus time. $\lambda_C = 10^{-7}\ s^{-1}$; $\lambda_O = 2 \times 10^{-7}\ s^{-1}$. See Table 1 for parameter values; $P_{out} = 0.90$ atm.

the substrate concentration is very low, indicating that no control is exerted by dissolved oxygen, nor (during most of the process) is the availability of substrate limiting.

For very small mass transfer coefficients (Figs. 10 and 11) this initial period is small relative to the total cleanup time, and the induction period is not observed on the time scale of the plot. In this case the amount of contaminant removed by biodegradation increases linearly with time because the process is controlled by oxygen transport. As mentioned earlier, this is in agreement with the field results reported by Urlings et al. (11), a biodegradation rate that is zero order in biomass and, following Hogg et al. (14), zero order in hydrocarbon. For these runs, even though oxygen concentration in the vapor phase remains close to 21%, the dissolved oxygen concentration is very low throughout the column, so all of the oxygen that is transferred from the gaseous to the aqueous phase is utilized for biodegradation.

For intermediate mass transfer coefficients (Fig. 9) an initial induction period may be observed with exponential increase in the amount of contaminant biodegraded up to 500,000 s (5.8 days), following which oxygen transport becomes controlling until the terminal portion of the remediation process, where substrate is limiting.

One interesting check on the program performance is to reproduce the change of the conditions that Hinchee and his collaborators (12,13) employed in the field to optimize biodegradation processes in the vadose zone during SVE. They reported a sharp increase (from 15–25 to 85–90%) in the relative contribution of bioremediation to the overall cleanup process by decreasing the gas flux tenfold. Results of runs identical to those presented in Figs. 7 to 11, except for the value of the well head pressure P_{out}, are reported in Figs. 12 to 16. (P_{out} = 0.90 atm for Figs. 7 to 11 versus 0.99 atm for Figs. 12 to 16.)

As expected, with large mass-transfer coefficients a tenfold decrease in the pressure gradient (which leads to a corresponding decrease in the gas flux) leads to a similar decrease in the contaminant stripping rate, indicating that the gaseous and aqueous phases are almost in equilibrium. For $\lambda_C = 10^{-3}$ and 10^{-4} s^{-1} the percent of VOC stripped during the first 300,000 s (3.5 days) decreases from nearly 60% (Figs. 7 and 8) to values of approximately 6% (Figs. 12 and 13). A very large increase in the final value of the relative contribution of biodegradation (from 8.7 to 88% for $\lambda_C = 10^{-3}$ s^{-1} and from 10 to 85% for $\lambda_C = 10^{-4}$ s^{-1}) is also observed, while the total cleanup time increases from 581,000 (6.7 days) to 659,000 s (7.6 days) ($\lambda_C = 10^{-3}$ s^{-1}) and from 639,000 s (7.4 days) to 1,097,000 s (12.7 days) ($\lambda_C = 10^{-4}$ s^{-1}).

However, while the curve corresponding to $\lambda_O = 2 \times 10^{-3}$ s^{-1} (Fig. 12) exhibits exponential behavior up to the point when substrate becomes

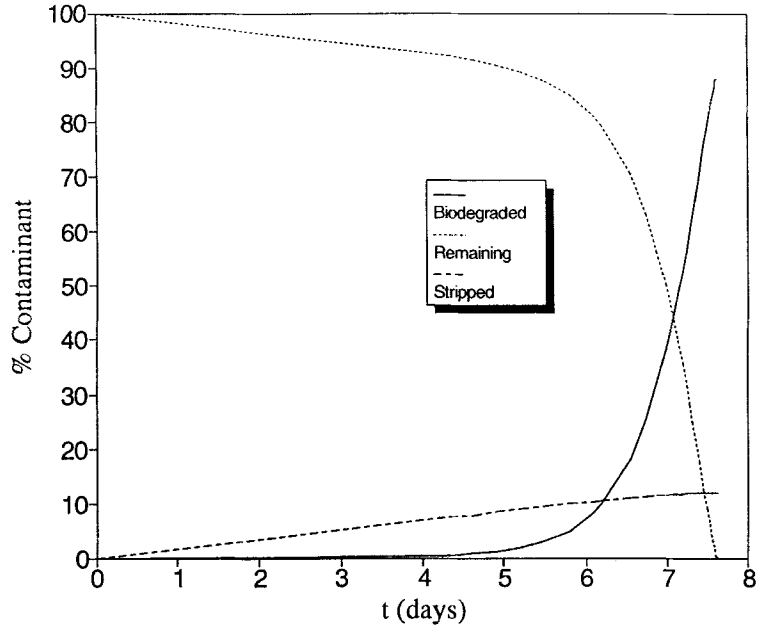

FIG. 12 Percentage of contaminant removal by stripping and biodegradation versus time. $\lambda_C = 10^{-3}\ s^{-1}$; $\lambda_O = 2 \times 10^{-3}\ s^{-1}$. See Table 1 for parameter values; $P_{out} = 0.99$ atm.

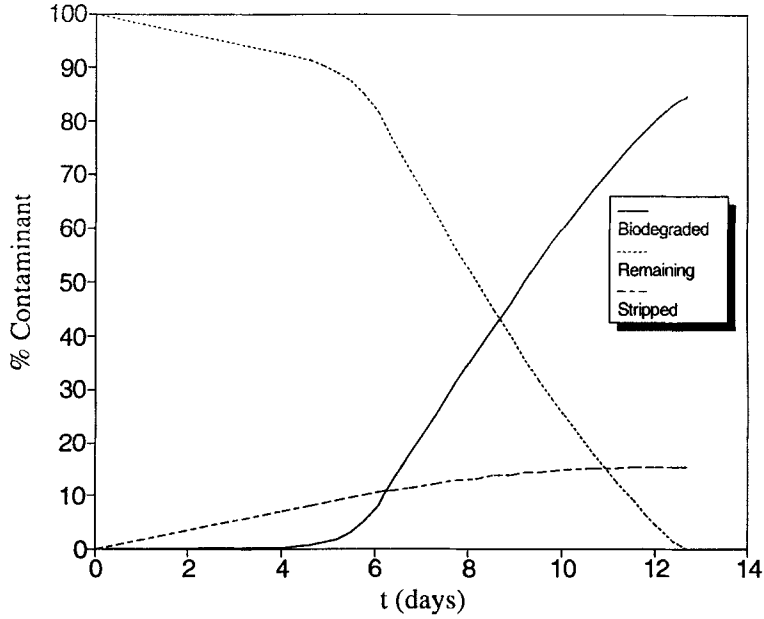

FIG. 13 Percentage of contaminant removal by stripping and biodegradation versus time. $\lambda_C = 10^{-4}\ s^{-1}$; $\lambda_O = 2 \times 10^{-4}\ s^{-1}$. See Table 1 for parameter values; $P_{out} = 0.99$ atm.

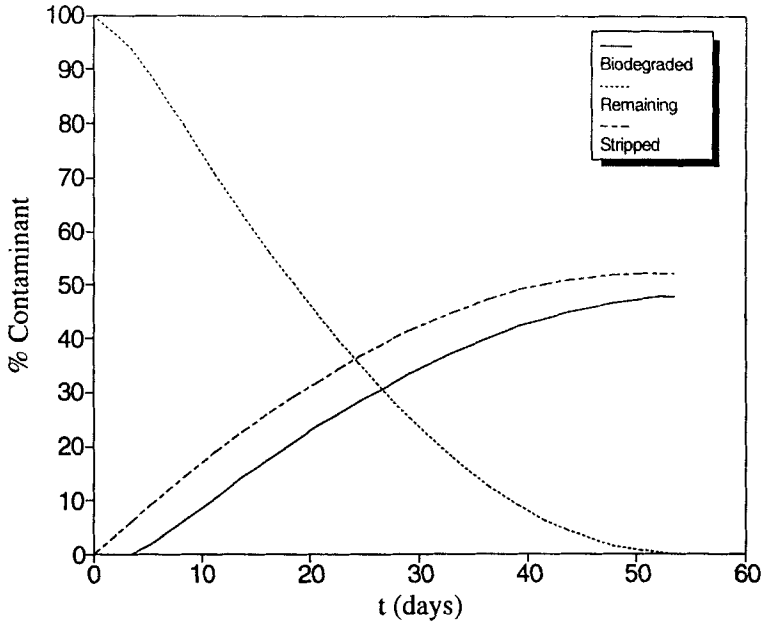

FIG. 14 Percentage of contaminant removal by stripping and biodegradation versus time. $\lambda_C = 10^{-5}\ s^{-1}$; $\lambda_O = 2 \times 10^{-5}\ s^{-1}$. See Table 1 for parameter values; $P_{out} = 0.99$ atm.

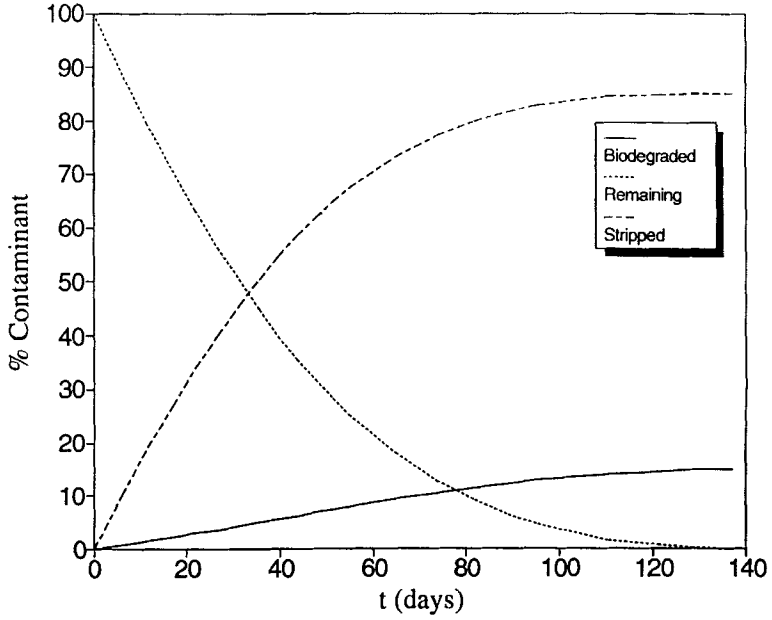

FIG. 15 Percentage of contaminant removal by stripping and biodegradation *versus time*. $\lambda_C = 10^{-6}\ s^{-1}$; $\lambda_O = 2 \times 10^{-6}\ s^{-1}$. See Table 1 for parameter values; $P_{out} = 0.99$ atm.

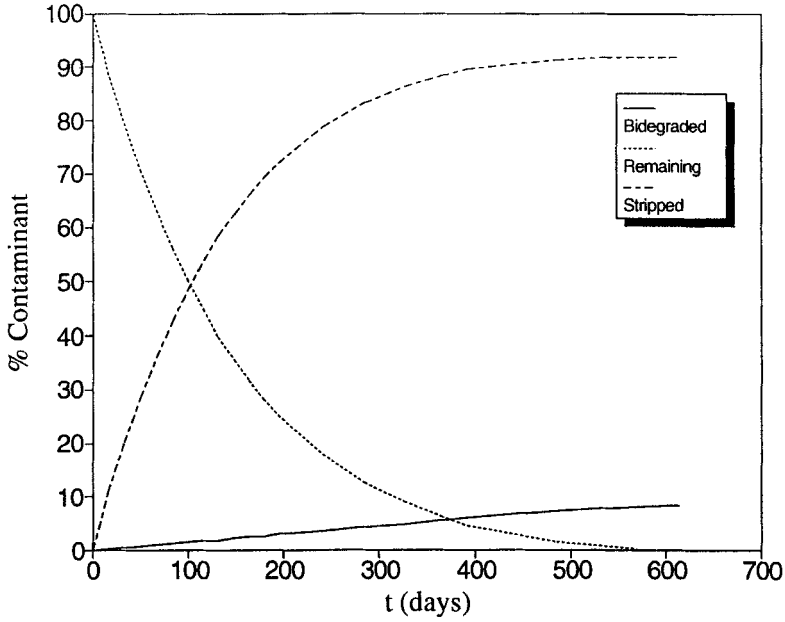

FIG. 16 Percentage of contaminant removal by stripping and biodegradation versus time. $\lambda_C = 10^{-7}\ s^{-1}$; $\lambda_O = 2 \times 10^{-7}\ s^{-1}$. See Table 1 for parameter values; $P_{out} = 0.99$ atm.

limiting, the curve obtained for $\lambda_O = 2 \times 10^{-4}\ s^{-1}$ (Fig. 13) shows exponential behavior only during the first 500,000 s (5.8 days), with a second stage of linear removal during which dissolved oxygen is controlling, with biodegradation occurring at a rate proportional to the rate of oxygen transfer from the gaseous phase to the aqueous phase. Then, close to the end of the cleanup process, a third stage is seen in which the substrate is limiting.

Obviously, when the pressure gradient is decreased, the same percentage drop in the gas flux will occur no matter what the values of the mass transfer coefficients. If, however, very low values ($\lambda_C = 10^{-7}\ s^{-1}$, $\lambda_O = 2 \times 10^{-7}\ s^{-1}$, Fig. 16) are used, the stripping process will be controlled mainly by transport from the stationary aqueous phase to the moving vapor stream, where contaminant concentration will be very low. Therefore, increasing the residence time of the gas in the column (or decreasing the gas flow rate) leads to a higher (but still low) contaminant concentration in the gas phase, and a smaller than expected decrease in the stripping rate occurs. Transport of oxygen from the gas stream to the stationary liquid will behave in similar fashion. Dissolved oxygen concentrations will

be close to zero in both cases, and a substantial increase in the ratio of oxygen utilized to oxygen introduced into the column will occur due to the longer gas residence time. As a result, cleanup time increases only from 43 to 53 million s (500 to 615 days) while the biodegradation contribution shows a slight increase (from 6.7% in Fig. 11 to 8.2% in Fig. 16).

Comparison of the results presented in Figs. 10 and 15 for mass transfer coefficients 10 times higher than those just discussed ($\lambda_C = 10^{-6}$ s^{-1} versus $\lambda_C = 10^{-7}$ s^{-1}) shows that, although mass transfer is still controlling both the stripping and the biological processes, it is not as stringently limiting as before. Therefore a substantial drop occurs in the stripping rate on decreasing the gas flow rate, and the overall cleanup time is only twice as large for the smaller flow rate [11.9 million s (138 days) in Fig. 15 versus 5.4 million s (62 days) in Fig. 10]. The fraction removed by biodegradation is twice as large (14.9%) at the lower gas flow rate as it is at the higher gas flow rate (7.6%).

Results obtained for larger values of the mass-transfer coefficients (in the intermediate range $\lambda_C = 10^{-5}$ s^{-1}, $\lambda_O = 2 \times 10^{-5}$ s^{-1}, Figs. 9 and 14) are in agreement with our previous discussion. The stripping rate is quite sensitive to the pressure gradient within the range examined, with roughly 75% stripped during the first 500,000 s (5.8 days) in Fig. 9 compared to only 10% for the same period in Fig. 14. On the other hand, biodegradation seems to proceed at almost the same rate, removing some 10% of the contaminant after approximately 1 million seconds (11.6 days). Since the total cleanup time increases when the gas flux decreases, the contribution of biodegradation increases, too (from 9.2 to 48%).

Thus, including mass transfer limitations from the bulk aqueous phase to the moving gas stream and vice versa in models describing the biological processes occurring during SVE allows one to model the most important features that have been described in the literature for field cases. Zero-order biodegradation kinetics are associated with control by oxygen transport from the gas stream to the aqueous solution, and a very important increase in the relative contribution of biodegradation results when the gas flux through the column is decreased.

HIGH-SPEED ALGORITHM DEVELOPMENT THROUGH APPROXIMATIONS

Run times with the model described above were determined on an IBM-AT clone computer (an MMG 286) with an 80286 processor and 80287 math coprocessor at 12 MHz. The program was written in TurboBASIC, and the integration of the differential equations was carried out by a standard predictor-corrector algorithm. As seen in Table 3, with such a ma-

chine extremely lengthy computation times are required even with a one-dimensional column model. Construction of faster algorithms would be helpful in developing practical column models even if faster machines were used, and is obviously essential if one is interested in two- or three-dimensional models even if one is using a 80386 or a 80486 based machine.

The most critical run-time problems occur for both the largest and smallest values of the mass-transfer rate constants, for different reasons. Very small increments of time are needed when using the larger constants, leading to a very large number of time steps per run. Larger time increments may be used as the mass transfer rate coefficient is decreased; however, longer cleanup times are needed, since cleanup times increase sharply for extremely low mass transfer rate constants. This, in turn, leads to a corresponding increase in the total calculation time. Several approximations in the algorithm were explored in order to shorten computation times and make the model a more convenient tool.

Local Equilibrium for the Contaminant Approximation

With large diffusion mass transfer rate constants, a local equilibrium model seems to be reasonable physically. In this section a version of the model is developed in which this approximation is made for the contaminant. The equations describing the system are modified as follows.

The local equilibrium approximation for substrate is given by

$$C^v = Kh_C C^s \tag{22}$$

Kh_C is the substrate (contaminant) Henry's constant. This assumption permits one to omit Eq. (11), since C^v can now be obtained from Eq. (22) as a function of C^s. The latter is obtained from the equation for contaminant removal:

$$\frac{\partial M}{\partial t} = \frac{\partial(vC^v + \omega C^s)}{\partial t} = (vKh_C + \omega)\frac{\partial C^s}{\partial t}$$

$$= v\left(-\frac{\partial(vC^v)}{\partial x}\right) + \omega\left(-n_c K \frac{O^s}{K_O + O^s}\frac{C^s B}{K_C + C^s}\right) \tag{23}$$

(advection) + (biodegradation)

Here M is the bulk contaminant concentration in soil. Equation (23) is readily transformed to

$$\frac{\partial C^s}{\partial t} = \frac{v\left(-\frac{\partial(vKh_C C^s)}{\partial x}\right) - \omega n_c K \frac{O^s}{K_O + O^s}\frac{C^s B}{K_C + C^s}}{vKh_C + \omega} \tag{24}$$

The model incorporating the assumption of local equilibrium for the contaminant is achieved by replacement of Eqs. (11) and (13) of the rigorous model with Eqs. (22) and (24). This change permits the use of larger time increments in the numerical integration for $\lambda_C = 10^{-3}\ s^{-1}$ (Δt = 40 s versus 0.75 s), and the computer time required to simulate a run is decreased from 29 to 1 hour. The results are essentially indistinguishable from the exact calculation. However, when this approximation is used for values of λ_C of $10^{-4}\ s^{-1}$ or less, excessively large deviations from the rigorous model occur.

Pseudostationary-State Approximation for the Vapor Phase of the Contaminant (C^v)

The bottleneck for quick calculations, once that the problem for large values of the diffusion mass transfer rate parameter is solved, is associated with much smaller mass transfer rate parameters. In previous work on SVE (31) that did not consider biodegradation, it was shown that a pseudosteady-state (stationary state) approximation allowed the use of substantially larger time increments in the numerical integration. Therefore the present model was modified to use a pseudosteady-state approximation for the vapor phase concentration of contaminant.

This approximation is indicated in

$$\frac{\partial C^v}{\partial t} = -\lambda_C \frac{\omega}{\nu}\left(\frac{C^v}{Kh_C} - C^s\right) - \frac{\partial(vC^v)}{\partial x} = 0 \tag{25}$$

in which the rate of contaminant diffusion from the aqueous phase to the vapor phase is set equal to the rate at which contaminant vapor is removed by advection, so that the vapor-phase concentration remains constant. This approximation is frequently used in analyzing complex chemical reactions in which intermediate species of short lifetime occur.

Equations (11) and (13) of the rigorous model may now be replaced by

$$\lambda_C \frac{\omega}{\nu}\frac{C^v}{Kh_C} + \frac{\partial(vC^v)}{\partial x} = \frac{\lambda_C \omega}{\nu} C^s \tag{26}$$

$$\frac{\partial C^s}{\partial t} = \frac{\nu}{\omega}\left(-\frac{\partial(vC^v)}{\partial x}\right) - n_C K \frac{O^s}{K_O + O^s}\frac{BC^s}{K_s + C^s} \tag{27}$$

One then forms the finite difference representations of Eqs. (26) and (27). This yields

$$C_i^v = \frac{\dfrac{v_{i-1}C_{i-1}^v}{\Delta x} + \dfrac{\omega\lambda_C}{\nu} C_i^s}{\dfrac{\nu_i}{\Delta x} + \dfrac{\omega\lambda_C}{\nu K h_C}} \tag{28}$$

$$\frac{\partial C_i^s}{\partial t} = \frac{v}{\omega \Delta x}(v_{i-1}C_{i-1}^v - v_i C_i^v) - n_C K \frac{O_i^s}{K_O + O_i^s}\frac{B_i C_i^s}{K_s + C_i^s} \quad (29)$$

Some results obtained with this approximation are shown in Table 4. The calculated cleanup times are not included, since the coincidence between the rigorous model and the approximation for the worst case is better than 0.1%. The most significant reduction in computer time is for a mass transfer rate parameter of 10^{-4} s^{-1} where the reduction is 75%. The least improvement is seen for $\lambda_C = 10^{-7}$ s^{-1}; the figure here is 10%. When larger time increments were used, the program crashed, giving inconsistent values for oxygen concentrations.

Pseudostationary-State Approximation for the Vapor-Phase Concentrations of Contaminant (C^v) and Oxygen (O^v)

In the previous runs, the vapor-phase oxygen concentration was observed to remain close to that of air for a few minutes after the cleanup process was started. The aqueous-phase oxygen concentration was found to remain almost constant after a substantial portion of the cleaning process had taken place. Therefore an attempt was made to develop a faster algorithm, working along the following lines. One may include the steady-state approximation for oxygen in the vapor phase and/or in the aqueous phase together with the steady-state approximation for the contaminant in the vapor phase. Thus, the next approximation to be examined is that in which the steady-state approximation is made for oxygen and contaminant, both in the vapor phase.

TABLE 4
Run Time Needed for the Rigorous Model Compared to the Pseudostationary Approximation for the Contaminant in the Vapor Phase

C^v pseudostationary approximation	Diffusion constants		Δt (s)	Run time (h), 99.996%
	λ_O (s^{-1})	λ_C (s^{-1})		
No	2×10^{-7}	10^{-7}	35	42.48
Yes	2×10^{-7}	10^{-7}	45	37.38
No	2×10^{-6}	10^{-6}	25	7.42
Yes	2×10^{-6}	10^{-6}	45	4.81
No	2×10^{-5}	10^{-5}	25	1.69
Yes	2×10^{-5}	10^{-5}	45	1.00
No	2×10^{-4}	10^{-4}	7.5	3.11
Yes	2×10^{-4}	10^{-4}	45	0.78

The steady-state approximation for oxygen in the vapor phase yields Eq. (30):

$$\frac{\partial O^v}{\partial t} = -\lambda_O \frac{\omega}{\nu}\left(\frac{O^v}{Kh_O} - O^s\right) - \frac{\partial(vO^v)}{\partial x} = 0 \tag{30}$$

which in the finite difference representation yields in turn

$$O_i^v = \left(\frac{v_{i-1}O_{i-1}^v}{\Delta x} + \frac{\lambda_O \omega}{\nu} O_i^s\right) \Big/ \left(\frac{v_i}{\Delta x} + \frac{\lambda_O \omega}{Kh_O \omega}\right) \tag{31}$$

Equation (31) replaces Eq. (12) for the calculation of the vapor-phase oxygen concentrations; the other equations are the same as in the previous model.

Important savings in computation time are achieved when both steady-state approximations are used, especially when one uses the very small mass transfer rate parameters which caused the greatest difficulties with the earlier calculations. Table 5 shows that for $\lambda_C = 10^{-7}\ s^{-1}$, almost no deviations from the results of the rigorous model occur when the time increments in the numerical integration of the approximate model are

TABLE 5
Run Time Needed for the Rigorous Model Compared to That Including Pseudostationary Approximations for the Contaminant and Oxygen in the Vapor Phase

C^v and O^v, pseudostationary approximation	Diffusion constants		Δt (s)	Run time (h)	99.996% cleanup time (h)
	λ_O (s^{-1})	λ_C (s^{-1})			
No	**2×10^{-7}**	**10^{-7}**	**35**	**42.48**	**1.2025×10^4**
Yes	2×10^{-7}	10^{-7}	125	13.34	1.2024×10^4
Yes	2×10^{-7}	10^{-7}	300	5.72	1.2024×10^4
Yes	2×10^{-7}	10^{-7}	350	4.84	1.1922×10^4
Yes	2×10^{-7}	10^{-7}	400	3.98	1.1158×10^4
No	**2×10^{-6}**	**10^{-6}**	**25**	**7.42**	**1.4944×10^3**
Yes	2×10^{-6}	10^{-6}	75	2.84	1.4943×10^4
Yes	2×10^{-6}	10^{-6}	100	2.10	1.4717×10^3
Yes	2×10^{-6}	10^{-6}	125	1.63	1.4093×10^3
No	**2×10^{-5}**	**10^{-5}**	**25**	**1.69**	**3.3707×10^2**
Yes	2×10^{-5}	10^{-5}	50	1.01	3.3697×10^2
Yes	2×10^{-5}	10^{-5}	75	0.70	3.2383×10^2
Yes	2×10^{-5}	10^{-5}	100	0.55	3.1047×10^2
No	**2×10^{-4}**	**10^{-4}**	**7.5**	**3.11**	**1.8463×10^2**
Yes	2×10^{-4}	10^{-4}	25	1.15	1.8467×10^2
Yes	2×10^{-4}	10^{-4}	75	0.52	1.8494×10^2
Yes	2×10^{-4}	10^{-4}	100	0.43	1.8364×10^2

below 300 s, and the deviations are below 1% when $\Delta t = 350$ s. These larger time increments decrease the computation time from 42 hours for the rigorous calculation (and 37 hours for the model using the steady-state approximation for the vapor-phase contaminant only) to only 4.8 hours when both contaminant and oxygen concentrations in the vapor phase are calculated by the steady-state approximation. Improvements in computing speed were observed for the entire range of mass transfer rate parameters for which the local equilibrium approximation was unsatisfactory.

Pseudostationary-State Approximation for Contaminant in the Vapor Phase (C^v) and for Oxygen in the Aqueous Phase (O^s)

If the steady-state approximation is made for oxygen in the aqueous phase, as well as for contaminant in the vapor phase, the maximum time increment in the numerical integration that gives consistent concentration values for mass transfer rate parameters in the range 10^{-4} to 10^{-7} s^{-1} is 40 s. Results are presented in Table 6. The algorithm includes the following modified equation:

$$\frac{\partial O^s}{\partial t} = \lambda_O \left(\frac{O^v}{Kh_O} - O^s \right) - n_O K \frac{O^s}{K_O + O^s} \frac{BC^s}{K_C + C^s} = 0 \qquad (32)$$

which yields

$$O_i^s = \frac{\dfrac{\lambda_O}{Kh_O} O_i^v}{n_O K \dfrac{1}{K_O + O_i^s} \dfrac{B_i C_i^s}{K_C + C_i^s} + \lambda_O} \qquad (33)$$

TABLE 6
Run Time Needed for the Rigorous Model Compared to the Pseudostationary Approximation for the Contaminant in the Vapor Phase and Oxygen in the Aqueous Phase Only

C^v and O^s, pseudostationary approximation	Diffusion constants		Δt (s)	Run time (h)	99.996% cleanup time (h)
	λ_O (s^{-1})	λ_C (s^{-1})			
No	**2×10^{-7}**	**10^{-7}**	**35**	**42.48**	**1.2025×10^4**
Yes	2×10^{-7}	10^{-7}	40	47.58	1.2025×10^4
No	**2×10^{-6}**	**10^{-6}**	**25**	**7.42**	**1.4944×10^3**
Yes	2×10^{-6}	10^{-6}	40	5.18	1.4955×10^4
No	**2×10^{-5}**	**10^{-5}**	**25**	**1.69**	**3.3707×10^2**
Yes	2×10^{-5}	10^{-5}	40	1.23	3.3758×10^2
No	**2×10^{-4}**	**10^{-4}**	**7.5**	**3.11**	**1.8463×10^2**
Yes	2×10^{-4}	10^{-4}	40	1.60	1.8484×10^2

This equation is solved iteratively for O_i^s. The improvements in computation time were not as large as were found in the earlier algorithms, so this approach was not pursued further.

Pseudostationary-State Approximation for Contaminant in the Vapor Phase (C^v) and for Oxygen in the Vapor (O^v) and Aqueous (O^s) Phases

One more attempt to obtain a faster algorithm was made; in this the steady-state approximation was made for the three variables O^v (vapor oxygen), O^s (dissolved oxygen), and C^v (vapor contaminant). The initial conditions for all the previous runs included the assumption that the oxygen concentration in the aqueous phase was zero. Therefore the rate of change of this variable with time at the beginning of the run was positive and relatively large, making the steady-state approximation for dissolved oxygen (O^s) fail during the initial phase of the run.

Some runs were also made with the initial condition that the dissolved oxygen in the aqueous phase was at saturation concentration. These results indicated slightly more biodegradation but also failed when the steady-state approximation for dissolved oxygen was included. This occurred for the following reason. Because the growth of biomass is controlled in the early stages of a run by the biomass concentration, biomass growth is exponential up to the time at which oxygen consumption in the aqueous phase is clearly more rapid than its replacement from the vapor phase. At this point a rather high negative slope occurs in the dissolved oxygen curve that makes the stationary-state approximation for dissolved oxygen invalid, inasmuch as this approximation assumes that the dissolved oxygen concentration is changing only quite slowly with time.

Therefore, the last attempt at algorithm improvement consisted in the implementation of a program with a changing algorithm. The program starts out using only the steady-state approximations for oxygen and contaminant in the vapor phase, and then, when the run has progressed to the point at which the oxygen concentration in the aqueous phase controls the growth of biomass, the third approximation (the steady-state approximation for dissolved oxygen) is also used.

With this method, when the mass transfer rate parameters λ_C and λ_O are extremely low, time increments Δt may be almost one hundred times larger than the maximum Δt values which can be used in the rigorous model. The resultant computation times for any values of the mass transfer rate parameters may be less than 1 hour, permitting the practical application of the model. Computation times are given in Table 7.

TABLE 7
Run Time and Calculated Cleanup Time Needed for the Rigorous Model Compared to the Pseudostationary Approximation for the Contaminant and Oxygen in the Vapor Phase and Oxygen in Aqueous Phase from the Moment That Oxygen Concentration Controls the Growth of Biomass

C^v, O^v, and O^s (in italics), pseudostationary approximation	Diffusion constants		Δt (s)	Run time (h)	Theoretical cleanup time (h)
	λ_O (s^{-1})	λ_C (s^{-1})			
No	**2×10^{-7}**	**10^{-7}**	**35**	**42.48**	**1.2025×10^4**
Yes	2×10^{-7}	10^{-7}	600	3.32	1.2024×10^4
Yes	2×10^{-7}	10^{-7}	900	2.27	1.2024×10^4
Yes	2×10^{-7}	10^{-7}	1500	1.33	1.2025×10^4
Yes	*2×10^{-7}*	*10^{-7}*	*3000*	*0.67*	*1.2018×10^4*
No	**2×10^{-6}**	**10^{-6}**	**25**	**7.42**	**1.4944×10^3**
Yes	2×10^{-6}	10^{-6}	350	0.64	1.4944×10^3
Yes	2×10^{-6}	10^{-6}	500	0.47	1.4835×10^3
Yes	*2×10^{-6}*	*10^{-6}*	*1000*	*0.25*	*1.4803×10^3*
No	**2×10^{-5}**	**10^{-5}**	**25**	**1.69**	**3.3707×10^2**
Yes	2×10^{-5}	10^{-5}	125	0.41	3.3701×10^2
Yes	*2×10^{-5}*	*10^{-5}*	*250*	*0.22*	*3.3458×10^2*
No	**2×10^{-4}**	**10^{-4}**	**7.5**	**3.11**	**1.8463×10^2**
Yes	2×10^{-4}	10^{-4}	100	0.32	1.8492×10^2
Yes	*2×10^{-4}*	*10^{-4}*	*200*	*0.19*	*1.8533×10^2*

Influence of the Number of Compartments into Which the Column Is Partitioned

One more series of runs was made in order to establish the influence of the number of compartments on the computations for an intermediate value of λ_C (10^{-5} s^{-1}). Selection of the number of compartments used to represent the column relates to numerical dispersion in the advective motion of components through the column; the smaller the number of compartments, the greater the numerical dispersion. One uses this numerical dispersion to model the axial dispersion actually occurring in the column.

The results are presented in Fig. 17. As can be seen, when the column is partitioned into 10 volume elements, the results differ by about 5% from those obtained when 60 volume elements are used. The uncertainty introduced by the choice of the number N of volume elements is evidently relatively small when compared to the impact of several of the other model parameters. Cleanup times always increase slightly with decreasing number of compartments used to represent the column, so a low choice of N errs on the conservative side. It is also noticeable that as N is increased,

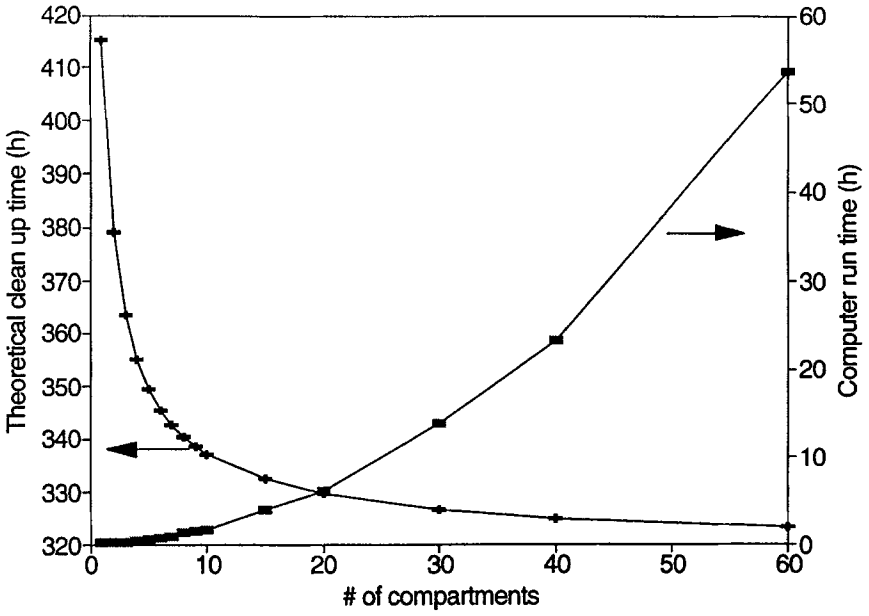

FIG. 17 Theoretical cleanup time and computer calculation time needed as a function of the number of divisions in the column model for the exact algorithm. $\lambda_C = 10^{-5}\ s^{-1}$, $\lambda_O = 2 \times 10^{-5}\ s^{-1}$.

the maximum admissible size of the time increment Δt decreases, which results in serious increases in computation time requirements. This point may also prove troublesome in the development of two-dimensional models.

FUTURE WORK

At this point we have developed what we believe to be a reasonably realistic, flexible, and usable mathematical model for bio-assisted soil vapor extraction. Mathematical modifications have been found which permit the running of the model on currently available microcomputers without undue time requirements. The model of necessity involves a rather large number of input parameters, the effects of only a few of which have been explored in the present paper. In future papers it is planned to investigate the impacts of other parameters on model output to determine the sensitivity of the modeling results to these parameters and give insight into which facets of the process might result in significant improvements in speed and efficiency of remediation. It is also planned to extend the

model to include the presence of nonaqueous phase liquid (NAPL) droplets from which organics must be dissolved before biodegradation can take place. The presence of NAPL is a common occurrence at hazardous waste sites, so this modification should increase the utility of the model significantly.

CONCLUSIONS

Soil vapor extraction is a technology that is becoming increasingly used for remediation of sites at which the vadose zone is contaminated with VOCs. Although it is a conceptually simple technology, optimal site-specific design and cleanup time estimation require mathematical modeling. Some field results indicate that models using the local equilibrium approximation may be overly optimistic, and that nonequilibrium effects may need to be considered (see Reference 31, for example, for comments on this). Such nonequilibrium processes may be responsible for poor improvements in the cleanup time when the gas flux through the soil is increased. Furthermore, costs of soil gas treatment may markedly increase as the contaminant is diluted in larger amounts of gas that must be treated before it can be discharged to the atmosphere.

Biodegradation processes have been observed in field studies during soil vapor extraction. These processes may produce important reductions in cleanup times, particularly if high percentage removals must be achieved, so they should be included in models describing the SVE of biodegradable VOCs. Oxygen mass transfer limitations from the gas to the aqueous phase may be expected. Inclusion of these kinetic limitations within a model, together with use of Monod kinetics for the description of the biological processes, permits one to simulate trends which are observed in experimental studies. Biodegradation rates of zero order with respect to contaminant and biomass (reported in the literature; see Reference 14) are associated with these limitations.

Very large increases in the percentage contribution of biodegradation to the cleanup process may result from a decrease in the gas flow rate. Under some circumstances this may lead to a relatively slight increase in the cleanup time, to substantially smaller volumes of exhausted soil gas to be treated, and to a substantial decrease in the total amount of contaminant which is air stripped (and therefore must be treated) for the same degree of remediation. Proper design and operation of such a facility therefore have the potential for significant savings.

The desired large percentage contribution of biodegradation may be limited by the availability of other nutrients, competition of other substrates, and/or toxic effects inhibiting the activity of the biomass. Although

the large number of parameters included in these models makes their use difficult on a precise predictive basis, sensitivity analysis of the most important variables is useful to understand the biodegradation phenomena promoted by SVE and to plan experiments to optimize the design of field-scale operations.

In order to develop algorithms of sufficient speed to permit their practical use on microcomputers in sensitivity studies and in the planning of experiments, several approximations were explored. For those cases in which large diffusion mass transport coefficients are expected (i.e., porous, highly permeable, relatively homogeneous media), the local equilibrium approximation for contaminant partitioning between the aqueous and the vapor phases yields results indistinguishable from those obtained with the exact algorithm and requires only 5% of the time needed by the exact algorithm. If the diffusion mass transport coefficients are expected to be small (media of highly heterogeneous permeability, high humic organic content, etc.), a variety of steady-state approximations is available. When the optimal of these approximations is used, results are obtained which are within 1% agreement with the exact calculations, and computer time requirements may be lower than 5% of that needed for use of the exact algorithm.

ACKNOWLEDGMENTS

We appreciate helpful discussions with Dr. J. J. Rodríguez during the development of the model. C.G.-L.'s contribution was made possible by a grant provided by the Spanish Ministry of Education and Science and the Fulbright Foundation.

REFERENCES

1. M. Russell, E. W. Colglazier, and M. R. English, *Hazardous Waste Remediation: The Task Ahead*, Waste Management Research and Education Institute, University of Tennessee, Knoxville, Tennessee, December 1991.
2. U.S. EPA, *Superfund Innovative Technology Evaluation (SITE) Program*, U.S. EPA Report EPA/540/8-91/005, 1991.
3. T. A. Pedersen and J. T. Curtis, *Soil Vapor Extraction Technology Reference Handbook*, U.S. EPA Report EPA/540/2-91/003, February 1991.
4. J. P. Stumbar and J. Rawe, *Guide for Conducting Treatability Studies under CERCLA: Soil Vapor Extraction*, U.S. EPA Report EPA/540/2-91/019a, September 1991.
5. R. E. Hinchee and R. F. Olfenbuttel (Eds.), *In Situ Bioreclamation. Applications and Investigations for Hydrocarbon and Contaminated Site Remediation*, Butterworth-Heinemann, Stoneham, Massachusetts, 1991.
6. R. E. Hinchee and R. F. Olfenbuttel (Eds.), *On Site Bioreclamation. Xenobiotic Hydrocarbon Treatment*, Butterworth-Heinemann, Stoneham, Massachusetts, 1991.

7. H. M. Freeman and P. S. Sferra (Eds.), *Innovative Hazardous Waste Treatment Technology Series. Vol. 3. Biological Processes*, Technomic Publishing Co., Lancaster, Pennsylvania, 1991.
8. J. Rawe, *Guide for Conducting Treatability Studies under CERCLA: Aerobic Biodegradation Remedy Screening. Interim Guidance*, U.S. EPA Report EPA/540/2-91/013a, July 1991.
9. R. E. Hinchee, D. C. Downey, R. R. Dupont, P. K. Aggarwal, and R. N. Miller, "Enhancing Biodegradation of Petroleum Hydrocarbons through Soil Venting," *J. Hazard. Mater.*, *27*, 315 (1991).
10. D. W. DePaoli, S. E. Herbes, and M. G. Elliot, "Performance of In Situ Soil Venting Systems at Jet Fuel Spill Sites," Appendix H of *Soil Vapor Extraction Technology Reference Handbook* (T. A. Pedersen and J. T. Curtis, Eds.), U.S. EPA Report EPA/540/2-91/003, February 1991.
11. L. G. C. M. Urlings, F. Spuy, S. Coffa, and H. B. R. J. van Vree, "Soil Vapor Extraction of Hydrocarbons. In Situ and On Site Biological Treatment," in *In Situ Bioreclamation. Applications and Investigations for Hydrocarbon and Contaminated Site Remediation* (R. E. Hinchee and R. F. Olfenbuttel, Eds.), Butterworth-Heinemann, Stoneham, Massachusetts, 1991.
12. R. R. Dupont, W. J. Doucette, and R. E. Hinchee, "Assessment of In Situ Bioremediation Potential and Application of Bioventing at a Fuel-Contaminated Site," in *In Situ Bioreclamation. Applications and Investigations for Hydrocarbon and Contaminated Site Remediation* (R. E. Hinchee and R. F. Olfenbuttel, Eds.), Butterworth-Heinemann, Stoneham, Massachusetts, 1991, p. 262.
13. R. N. Miller, C. C. Vogel, and R. E. Hinchee, "A Field Scale Investigation of Petroleum Hydrocarbon Biodegradation in the Vadose Zone Enhanced by Soil Venting at Tyndall AFB, Florida," in *In Situ Bioreclamation. Applications and Investigations for Hydrocarbon and Contaminated Site Remediation* (R. E. Hinchee and R. F. Olfenbuttel, Eds.), Butterworth-Heinemann, Stoneham, Massachusetts, 1991, p. 283.
14. D. S. Hogg, R. J. Burden, and P. J. Riddell, "In Situ Vadose Zone Bioremediation of Soil Contaminated with Non-Volatile Hydrocarbons," HMCRI R & D Conference, San Francisco, February 1992.
15. S. Kayano and D. J. Wilson, "Soil Clean Up by *in-situ* Aeration. X. Vapor Stripping of Mixtures of Volatile Organics Obeying Raoult's Law," *Sep. Sci. Technol.*, *27*, 1525 (1992).
16. R. C. Borden and P. B. Bedient, "Transport of Dissolved Hydrocarbons Influenced by Oxygen-Limited Biodegradation. I. Theoretical Development," *Water Resour. Res.*, *22*, 1973 (1986).
17. K. T. B. MacQuarrie, E. A. Sudicky, and E. O. Frind, "Simulation of Biodegradable Organic Contaminants in Groundwater. I. Numerical Formulation in Principal Directions," *Ibid.*, *26*, 207 (1990).
18. M. A. Widdowson, F. J. Molz, and L. D. Benefield, "A Numerical Transport Model for Oxygen- and Nitrate-Based Respiration Linked to Substrate and Nutrient Availability in Porous Media," *Ibid.*, *24*, 1553 (1988).
19. M. A. Widdowson and C. M. Aelion, "Applications of a Numerical Model to the Performance and Analysis of an In Situ Bioremediation Project," in *In Situ Bioreclamation. Applications and Investigations for Hydrocarbon and Contaminated Site Remediation* (R. E. Hinchee and R. F. Olfenbuttel, Eds.), Butterworth-Heinemann, Stoneham, Massachusetts, 1991, p. 227.
20. B. E. Sleep and J. F. Sykes, "Biodegradation of Volatile Organic Compounds in Porous Media with Natural and Forced Gas-Phase Advection," in *In Situ Bioreclamation.*

Applications and Investigations for Hydrocarbon and Contaminated Site Remediation (R. E. Hinchee and R. F. Olfenbuttel, Eds.), Butterworth-Heinemann, Stoneham, Massachusetts, 1991, p. 245.

21. L. Semprini and P. McCarty, "Comparison between Model Simulations and Field Results for In Situ Biorestoration of Chlorinated Aliphatics: Part 1. Biostimulation of Methanotrophic Bacteria," *Ground Water, 29*, 365 (1991).
22. L. Semprini and P. McCarty, "Comparison between Model Simulations and Field Results for In Situ Biorestoration of Chlorinated Aliphatics: Part 2. Cometabolic Transformations," *Ibid., 30*, 37 (1992).
23. F. Spuy, S. Coffa, C. Pijls, and L. G. C. M. Urlings, "In Situ Vapour Extraction of Contaminated Soils," in *Third Forum on Innovative Hazardous Waste Treatment Technologies. Domestic and International*, Dallas, Texas, June 11–13, 1991, U.S. EPA Report EPA/540/2-91/015, 1991, p. 82.
24. J. S. Gierke, N. J. Hutzler, and D. B. McKenzie, "Vapor Transport in Unsaturated Soil Columns: Implications for Vapor Extraction," *Water Resour. Res., 28*, 323 (1992).
25. D. J. Wilson, A. N. Clarke, and J. H. Clarke, "Soil Clean Up by *in-situ* Aeration. I. Mathematical Modeling," *Sep. Sci. Technol., 23*, 991 (1988).
26. R. C. Reid, J. M. Prauswitz, and T. K. Sherwood, *The Properties of Gases and Liquids*, 3rd ed., McGraw-Hill, New York, 1977, p. 576.
27. M. D. Lee, J. T. Wilson, and C. H. Ward, "Microbial Degradation of Selected Aromatics at a Hazardous Waste Site," *Dev. Ind. Microbiol., 25*, 557 (1984).
28. S. Dhawan, L. T. Fan, L. E. Erickson, and P. Tuitemwong, "Modeling Analysis and Simulation of Bioremediation of Soil Aggregates," *Environ. Prog., 10*(4), 251 (November 1991).
29. I. Bossert and R. Bartha, "The Fate of Petroleum in Soil Ecosystems" in *Petroleum Microbiology* (R. M. Atlas, Ed.), Macmillan, New York, 1984.
30. R. E. McKinney, *Microbiology for Sanitary Engineers*, McGraw-Hill, New York, 1962.
31. J. M. Rodriguez-Maroto and D. J. Wilson, "Soil Clean Up by *in-situ* Aeration. VII. High-Speed Modeling of Diffusion Kinetics," *Sep. Sci. Technol., 26*, 743 (1991).
32. D. C. DiGiulio, J. S. Cho, R. R. Dupont, and M. W. Kemblowski, "Conducting Field Tests for Evaluation of Soil Vacuum Extraction Application, " in *Proceedings of the 4th National Outdoor Action Conference on Aquifer Restoration, Ground Water Monitoring and Geophysical Methods*, Las Vegas, Nevada, May 14–17, 1990, p. 587.
33. S. E. Strand, R. M. Seamons, A. D. Bjelland, and H. D. Stensel, "Kinetics of Methane Oxidizing Biofilms for Degradation of Toxic Organics," *Water Sci. Technol., 20*, 167 (1988).

Received by editor July 12, 1993